Solid-State ^{1}H NMR Study on Chemical Cross-Links, Chain Entanglements, and Network Heterogeneity in Peroxide-Cured EPDM Rubbers

Ramona A. Orza,[†,§] Pieter C. M. M. Magusin,*[,†] Victor M. Litvinov,[‡,§] Martin van Duin,[‡] and M. A. J. Michels[†,§]

Eindhoven University of Technology, P.O. Box 513, 5600 MB Eindhoven, The Netherlands, DSM Research, P.O. Box 18, 6160 MD Geleen, The Netherlands, and Dutch Polymer Institute, P.O. Box 902, 5600 AX Eindhoven, The Netherlands

Received May 4, 2007; Revised Manuscript Received September 28, 2007

ABSTRACT: Peroxide-cross-linked ethylene−propylene−(diene) rubbers, EP(D)M, have complex network structures with various types of chemical cross-links as well as both temporary and trapped chain entanglements. To obtain a detailed picture of the respective contributions of these different types of cross-links and entanglements to the total network density, solid-state ^{1}H NMR relaxometry and spectroscopy have been applied to a series of peroxide-cured EPDM with systematic variation of the peroxide and diene contents. The effective Hahn-echo decay time T_2 reflects the volume-average network density, which correlates well to mechanical properties, such as torque and modulus, and linearly depends on the initial peroxide content for the compositions probed. The slope reflects the peroxide-induced chemical cross-links. The chain-entanglement density that is estimated from the intercept agrees with published neutron scattering values. The observed differences in cross-link density between EPDM an EPM are consistent with the double bond conversion estimated from magic angle spinning ^{1}H NMR and Raman spectra. By comparing T_2 relaxation times in solid and swollen EPDM, we can distinguish between the contributions of temporary and trapped entanglements. The shapes of the Hahn-echo decays suggest strong network heterogeneity, which has also been probed by use of double-quantum-filtered T_2 relaxometry.

1. Introduction

Ethylene−propylene (EPM) copolymers and ethylene−propylene−diene (EPDM) terpolymers are among the most versatile synthetic rubbers. The ethylene and propylene comonomers result in a saturated polymer backbone in which the nonconjugated diene monomers are randomly distributed. The properties of these elastomers can be modified by adjusting the copolymer structure, including the ethylene/propylene ratio and the content of diene, the molecular weight (distribution), and the degree of branching. In commercial EPDM terpolymers, the diene is mainly ethylidene norbornene (ENB) or dicyclopentadiene (DCPD) (Figure 1). Incorporation of the diene introduces unsaturation in EPDM and enables sulfur vulcanization and enhances peroxide cross-linking.

The hydrocarbon character of EPDM in combination with the high molecular weight explains the ability to accommodate large quantities of fillers and oil without creating processing instabilities and unacceptable loss of physical properties. Because of the saturated main chain, EPDM provides excellent resistance to oxygen, ozone, heat, and irradiation without the need for large quantities of stabilizers. As a result, EPDM is suitable for outdoor and high-temperature applications. EPDM has found use in widespread applications, ranging from automotive sealing (windows, door, and trunk) to building and construction (profiles, roof sheeting, pipes, hoses, and seals).

Elastomers are usually cross-linked to have the best performance, such as high elasticity, high tensile strength, and good resistance to solvents. Traditionally, sulfur vulcanization is applied, which however suffers from S−S bond cleavage at elevated temperatures. Peroxide cure results in more thermally stable networks.

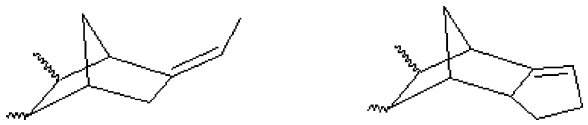

Figure 1. Chemical structures of EPDM third monomers.

The commonly accepted reaction scheme for peroxide cure is shown in Figure 2.[1] At elevated temperatures the peroxide decomposes into radicals, which can react with the polymer chains by abstraction of hydrogen atoms to produce macroradicals. Combination of these macroradicals leads to cross-linking between polymer chains. Peroxide cure of EPM is relatively inefficient, but the incorporation of diene strongly enhances peroxide cure. In EPDM, the radicals can react with the residual double bonds of dienes in two ways: abstraction of allylic hydrogen atoms or addition to the double bond. This second route is favored when the double bond is terminal, while an internal double bond tends to react more via H abstraction. The radicals produced via the addition reaction undergo hydrogen transfer, yielding new macroradicals that can add to another terminal bond to produce another cross-link without radical destruction. In this case, the peroxide cross-linking efficiency is relatively high.[2]

The characterization of cross-linked elastomers is of great scientific and technological interest.[3−5] It enables the understanding of the network formation in terms of rubber molecular structure, cure recipe, and conditions, and it allows the correlation of macroscopic properties with the network structure. The cross-link density is one of the main characteristics of a cross-linked rubber, with network heterogeneity as a secondary feature.

* To whom correspondence should be addressed. E-mail: p.c.m.m.magusin@tue.nl.
† Eindhoven University of Technology.
‡ DSM Research.
§ Dutch Polymer Institute.

10.1021/ma071015l CCC: $37.00
Published on Web 11/15/2007

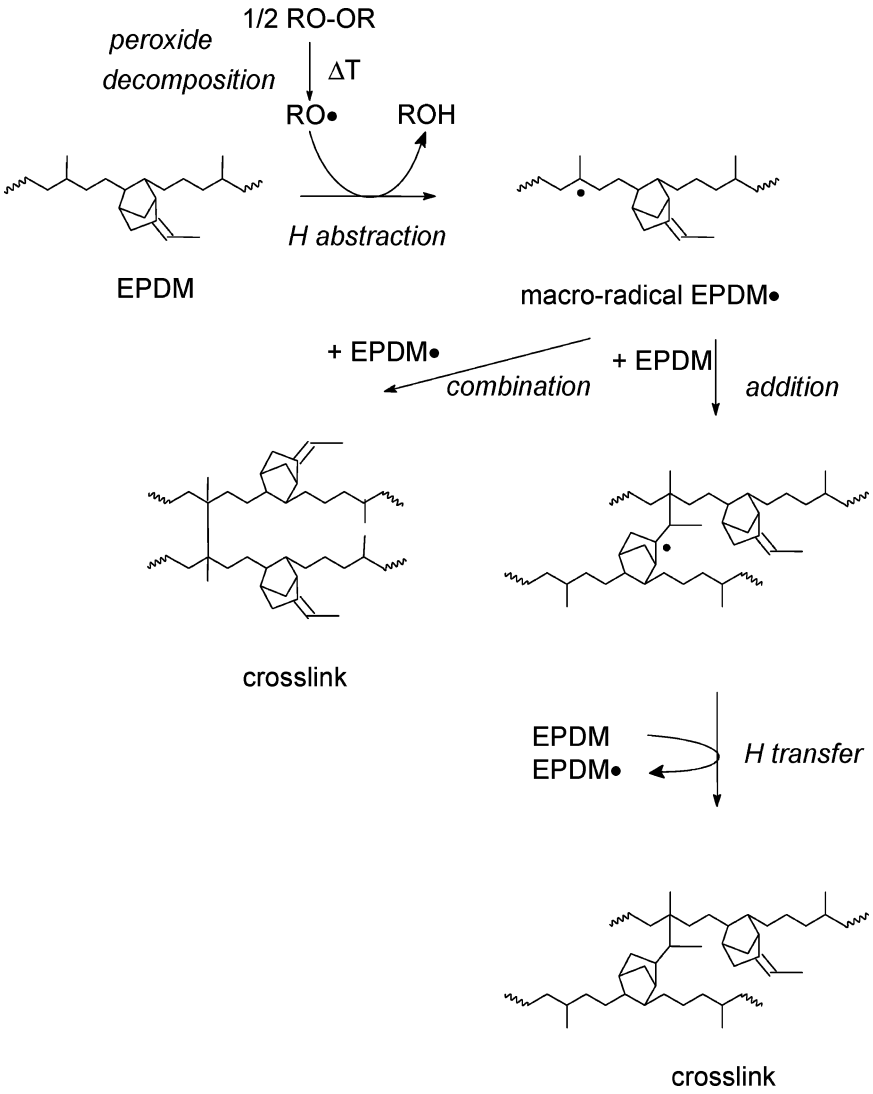

Figure 2. Mechanism of peroxide curing of EPDM.

Solid-state ^{1}H NMR transverse magnetization relaxometry yields detailed insight into the network structure of cross-linked rubbers.[6−11] For highly mobile polymer chains, as in rubbers, the transverse relaxation is slow and the corresponding T_2 value is long. At temperatures far above the glass transition temperature, T_g, the chain motion in cross-linked polymers is restricted by the network junctions, causing a high-temperature plateau in the temperature dependence of T_2. At this high-temperature limit, the T_2 value mainly depends on the anisotropy of the chain motions, which is controlled by the chain lengths between the network junctions. As a result, information on the network structure and defects can be obtained from ^{1}H NMR relaxometry.[12] The shorter the chain length between cross-links the higher is the anisotropy of chain motion and lower is the T_2 value at the plateau, T_2^{pl}.

The aim of this work is to study the various aspects of peroxide cure of EPDM: (i) cross-linking chemistry, (ii) the effect of the EPDM composition and the amount of peroxide on the total cross-link density and the contribution of different types of chemical cross-links and chain entanglements to the total network density, and (iii) network heterogeneity. Different methods are used for this purpose, i.e., ^{1}H NMR T_2 relaxation experiments, ^{1}H NMR spectroscopy, FT-Raman spectroscopy, and double-quantum (DQ) edited T_2 relaxation experiments. Applied to an array of EPDM grades, this yields a consistent picture in terms of conversion and network density.

Table 1. Chemical Structure of EPDMs Used

diene type		ENB	ENB	ENB	DCPD
diene content (wt %)	0	1.9	4.5	9.0	4.5
ethylene content (wt %)	49	54	52	48	55

2. Experimental Section

2.1. Sample Composition and Preparation. The chemical compositions of the studied EPM and EPDM grades are given in Table 1. The EPDM/peroxide mixtures have been selected to cover a wide range of both diene termonomer and peroxide content. Amorphous EPDMs (ethylene contents below 55%) with both ENB and DCPD as dienes were used. The samples have been cured with different amounts of di(*tert*-butyl peroxy isopropyl)benzene (BPB). BPB was used as a 40% masterbatch (Perkadox14-40 MB-GR from Akzo Nobel). The peroxide levels are given in parts per hundred rubbers (phr), which is a common practice in rubber technology. However, for a more scientific interpretation, parts per hundred BPB has been converted into millimoles of peroxide function per kilogram of EPDM, taking into account the purity (40% BPB on 60% of whitening silica and EPDM), the molecular weight (338.5 g/mol), and the functionality (two peroxide functionalities in one BPB molecule). Each type of EPDM was cured with different amounts of peroxide masterbatch: 1.25, 2.5, and 5 phr, and for EPM an additional concentration of 10 phr was used. The constituents were mixed in an open mill and vulcanized in a hot press at 175 °C for 17 min. For some NMR experiments, samples were swollen in $C_2D_2Cl_4$ from Merck.

2.2. ^{1}H NMR Hahn-Echo Experiments. The ^{1}H transverse magnetization relaxation of the cross-linked EPDM as such and after swelling in $C_2D_2Cl_4$ was measured on a Bruker Minispec MQ-20 spectrometer operating at a ^{1}H frequency of 20 MHz. This spectrometer was equipped with a BVT-3000 variable temperature unit. All experiments were performed at 90 °C.

The decay of the transverse magnetization was measured with the Hahn-echo pulse sequence (HEPS): $90°_x-t_{HE}-180°_y-t_{HE}-$[acquisition of the amplitude of an echo maximum $A(t)$], where $t_{HE} \geq 35$ μs. This pulse sequence eliminates the magnetic field and chemical shift inhomogeneity and allows for robust and quantitative measurements. An echo signal is formed with a maximum at time $t = 2t_{HE} + (t_{90}/2) + (t_{180}/2)$ from the beginning of the first pulse, where t_{90} and t_{180} are the durations of the 90° and 180° pulses, respectively. By variation of the pulse spacing in the sequence, the amplitude of the transverse magnetization is measured as a function of the echo time $2t_{HE}$.

For measurements in the swollen state, a controlled amount of $C_2D_2Cl_4$ was added to the sample and allowed to equilibrate overnight. $C_2D_2Cl_4$ was used because of its high boiling point (146.2 °C) that enables NMR experiments for swollen samples at 90 °C without solvent evaporation.

The high-temperature limit value T_2^{pl} is a measure for the cross-link density. The T_2^{pl} value is related to the number of statistical segments between chemical and physical network junctions.[5,12] The mean molar mass M_w of the chains between the network junctions with fixed positions at the 10^{-3} s timescale follows from T_2^{pl} according to

$$M_w = \frac{T_2^{pl}}{aT_2^{rl}} C_\infty \frac{M_u}{n} \quad (1)$$

where M_u and n are the average mass and the number of backbone bonds per elementary chain unit, respectively, and C_∞ and a are model parameters. The former represents the number of rotating backbone bonds in the statistical segment of an infinite polymer chain and equals to 6.62 at 363 K for an alternating EPM.[13] The latter relates the mechanism of local segment motion to the resulting NMR relaxation, and more precisely, it depends on the angle between the polymer segment axis and the internuclear vector for the nearest ^{1}H spins in the main chain. For polymers containing aliphatic ^{1}H atoms in the main chain, the coefficient $a \sim 6.2 \pm 0.7$.[5,6] The rigid-limit value T_2^{rl} at temperatures far below T_g is related to the strength of the intrachain ^{1}H$-^1$H interactions in the rigid lattice.[5,13] For EPDM swollen in tetrachloroethane, the T_2^{rl} value equals 10.4 ± 0.2 μs at 140 K.[13] The total network density D_{tot} is inversely proportional to M_w,

$$D_{tot} = \frac{2}{fM_w} \quad (2)$$

where f is the functionality of the network junctions, e.g., $f = 4$ for pairwise-connected polymer chains.

2.3. ^{1}H Double-Quantum-Filtered T_2 Experiments. To get insight into the heterogeneous nature of the Hahn-echo decays, the underlying Hahn-decay components have been separated by use of a double-quantum (DQ)-filtered HEPS. DQ coherence is generated faster in rigid than in mobile polymer regions. Therefore, on the basis of their different response to the DQ filter, local polymer regions with different chain mobility can be selected and their Hahn-echo decays can be measured separately. The pulse sequence is shown in Figure 3. The subscripts EX, EV, RE, and DE stand for excitation, evolution, reconversion, and detection periods, respectively. The first three pulses $90°_\phi-(\tau_{EX}/2 - 180°_\phi)-(\tau_{EX}/2 - 90°_{-\phi})$ separated by time delays $\tau_{EX}/2$ convert the longitudinal spin polarization to the DQ coherence. The 180° refocusing pulse eliminates the effects of frequency offsets, resulting from chemical shift heterogeneity and susceptibility effects.[14] The second three pulses $90°_\psi-(\tau_{EX}/2 - 180°_\psi)-(\tau_{EX}/2 - 90°_{-\psi})$ either yield a further loss of polarization or reconvert the DQ coherence back to polarization depending on the relative phase shift $\phi-\psi$. By means of a proper phase cycle, only magnetization components produced by the excitation and the reconversion are selectively accumulated. With the appropriate values for the excitation and reconversion times, polymer regions with varying mobility can be selected. The time interval τ_{EV} was set to 5 μs. Between the DQ filter and the actual Hahn-echo pulses, a z-filter time τ_{DE} of 5 ms is applied to eliminate unwanted coherences arising from pulse imperfections, which could otherwise perturb the acquired NMR signal. Another role of this interval is to promote isotropic mixing of the z magnetization, resulting from the double-quantum reconversion. The double-quantum buildup at short excitation times ($10^{-6}-10^{-5}$ s) depends on the orientation of the (residual) dipolar coupling tensors with respect to the magnetic field B_0. For instance, the magnetization of the chain segments with dipole tensors oriented along B_0 are enhanced relative to those with tensors under the magic angle. Therefore, a sufficiently long delay time τ_{DE} is required for a proper redistribution of the magnetization between the chains with different direction of the end-to-end vectors with respect to the B_0. This redistribution of the magnetization is caused by a combination of chain mobility and ^{1}H NMR spin diffusion at the nanometer scale. Test experiments with different τ_{DE} times have shown that 5 ms was sufficient for local isotropic redistribution of the magnetization over all chain segment orientations without losing the ability to discriminate between the rigid and mobile polymer regions at a larger scale length.[15] By a proper choice of the excitation and reconversion times, i.e., $\tau_{EX} = \tau_{RE}$, the decay of the transverse magnetization of phases with different molecular mobility and, consequently, with different strengths of the dipole−dipole interactions can be selected.[16−21]

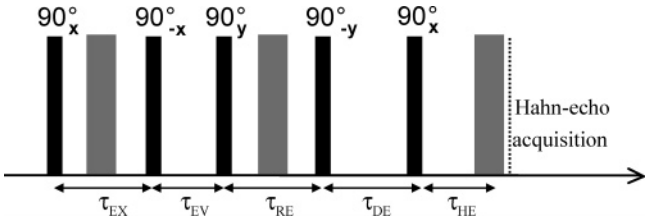

Figure 3. Double-quantum edited Hahn-echo pulse sequence. 180° pulses are shown by gray bars.

The DQ-HEPS experiments were performed at 90 °C for the samples, as such and after swelling, at two different solvent concentrations (≈40 and ≈80 vol %).

2.4. ^{1}H NMR Spectroscopy. Magic angle spinning (MAS) ^{1}H NMR spectra were recorded on a Bruker DMX 500 spectrometer at a resonance frequency of 500 MHz. A 4 mm probe head was used with a MAS rate of 12.5 kHz. The spectra were acquired by means of a single-pulse excitation with a 90° pulse of 5 μs and a recycling delay time of 5 s. The experiments were performed at 90 °C.

2.5. Raman Spectroscopy. In order to determine the conversion of the residual unsaturation of the EPDM diene, Raman spectroscopy was performed on 2 mm thick EPDM coupes using a Raman Station (Avalon Instruments, Belfast, Northern Ireland) equipped with a 785 nm laser and a dispersive detector. Spectra were recorded with a resolution of 2 cm^{-1}, and the typical measurement time per sample was 10 min. The ratio of the ENB unsaturation peak height at 1688 cm^{-1} to a reference peak height at 1438 cm^{-1} (caused by the $>CH_2$ scissoring) is calculated after the baseline subtraction height in the areas of interest. Subsequently, the conversion is calculated from the change in the peak height ratio.

2.6. Mechanical Measurements. The compounds were (fully) cured in an MDR 2000 E rheometer from Dynisco (formerly Alpha Technologies) at 175 °C to measure the increase in torque during curing, according to ISO 6502. The compounds were also cured in a hot press at 175 °C for appropriate cure times and characterized for hardness, tensile strength, and compression set at 23 and 70 °C according to DIN 53505, ISO 37, and ISP 815 methods, respectively.[22] For the modulus at 100% elongation, the tensile strength,

and the elongation at break, the median value of five experiments is presented.

3. Results and Discussion

3.1. Network Heterogeneity of Peroxide-Cured EPDM Rubber. ^{1}H NMR Hahn-echo decays of cross-linked elastomers can often be empirically described in terms of two or three exponentials. A quantitative analysis of the Hahn-echo decay for cross-linked elastomers is not always straightforward due to the structural heterogeneity of rubbery networks, and the fact is that even for a homogeneous polymer network with only chain entanglements, like polyethylene in the melt, the transverse magnetization loss is not intrinsically monoexponential.[8,23−27] The structural heterogeneity is related to the different types of network junctions, i.e., chemical network junctions, temporary and trapped chain entanglements, and the molar mass distribution of the network chains, and network defects, such as dangling chain ends and chains loops.[6] A complex network topology is expected for peroxide-cured rubbers because there are several types of chemical reactions producing cross-links; radical-induced chain scission may occur, and there may be concentration gradients of peroxide in the rubbery matrix caused by the low peroxide solubility. T_2 relaxometry can provide information on the heterogeneous distribution of network junctions. The sensitivity of the T_2 experiments to the molecular scale heterogeneity is related to the local origin of the relaxation process, which is predominantly governed by the near-neighbor environment and intrachain effects for T_2 relaxation at temperatures well above T_g. Therefore, the *submolecules* concept can be used to describe the relaxation behavior.[8] This concept treats polymer chains as strings of beads, submolecules, with effective overall orientation, mobility, and NMR features derived from the time-average configuration of short chain segments. The inequivalence between protons within the submolecules, e.g., methyl, methylene, and methine protons for EPDM, is neglected. These submolecules are part of longer chain segments between the chemical and physical network junctions, which restrict their mobility. The shorter the distance between network junctions the more restricted the motion of the beats and the faster the T_2 relaxation. In this coarse-grain picture, the total T_2 relaxation decay for a heterogeneous elastomer is the sum of the decays from different submolecules with different motional anisotropy, as result of distribution in network chain lengths, chain loops, and dangling chain ends. Indeed, nonexponential Hahn-echo decays have been observed for all EP(D)M samples in this study as illustrated in Figure 4. The underlying heterogeneity is demonstrated in DQ-filtered relaxation experiments (Figure 5), a method which was recently developed.[28] By control of the DQ-filter parameter, i.e., the DQ-quantum excitation and reconversion times, the Hahn-echo decays of chain segments with large or small motional anisotropy, i.e., with either more restricted or less restricted chain mobility, respectively, can be selectively observed. For the solid (nonswollen) materials, the DQ-filtered T_2 relaxation decays have been measured at three excitation times, $\tau_{EX} = 80$, 500, and 1100 μs, and are compared with the nonfiltered overall decay (Figure 5). The least mobile segments are selected by the 80 μs filter, whereas the DQ filter of 1100 μs selects the highly mobile segments, such as longer network chains and chain defects. As expected, the most restricted segments show faster Hahn-echo decays than the least restricted ones. For non-cross-linked EPDM, the various DQ-filtered decays are relatively close to each other, indicating that the sample is rather homogeneous. There is only limited T_2 heterogeneity associated with the natural entanglement distribution, dangling chain ends, and chemical inequivalence among the EPDM protons. The additional heterogeneity in chain mobility caused by peroxide cross-linking is evident from the broader range of relaxation timescales for cross-linked EPDM at various DQ-filter times.

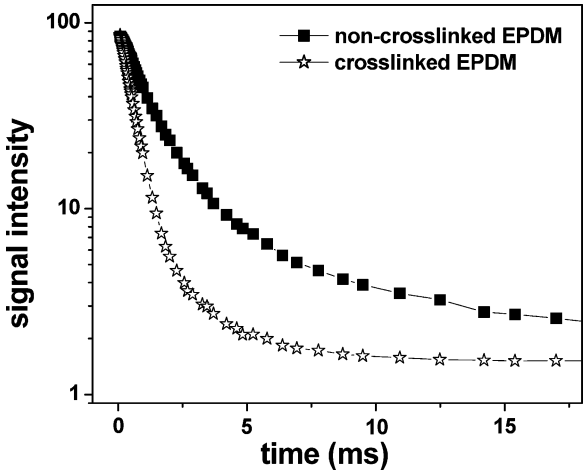

Figure 4. ^{1}H NMR T_2 relaxation decay for peroxide-cured EPDM with the highest peroxide and ENB content before and after cross-linking (9% ENB containing EPDM with 5 phr peroxide).

Although powerful as a semiquantitative method to probe the heterogeneity of chain motions, DQ-filtered T_2 relaxation measurements do not yield accurate quantitative information. We therefore fall back on the robust Hahn-echo decay method. With the possible flaws regarding the validity of its underlying polymer model and NMR theory, the Hahn-echo method has proven its validity in practice for a wide range of industrially relevant rubbers.[29] Due to the complex nature of peroxide-cross-linked rubbers, it will not be attempted to set up a detailed realistic model to analyze the observed relaxation curves. Instead, the T_2 relaxation decay is analyzed in terms of a phenomenological model with three exponentials $R(t) = \Sigma f_k \exp(-t/T_2^k)$ with fractions f_k of the respective components in the fit. The mean decay time, T_2^{av}, defined as $(\Sigma f_k/T_2^k)^{-1}$ is the weighted average of the exponential decays and is related to the volume-averaged cross-link density in the samples. Although T_2^{av} is determined from a fit of the curve as a whole, in the context of the triexponential model it is directly related to the initial slope.

The T_2 decays of non-cross-linked EPDM with the highest diene content and its vulcanizate are compared in Figure 4. Obviously, cross-linking causes a large decrease in the decay time, because chemical cross-links impose severe restrictions on the chain mobility compared to the entangled melt.

3.2. Total Network Density. The total network density D_{tot} of the heterogeneous EPDM network after peroxide cross-linking follows from the mean molar mass M_w of the chains between the network junctions (chemical cross-links and chain entanglements), which is calculated from $1/T_2^{av}$ (eq 2). Figure 6 shows the plot of D_{tot} at varied peroxide content for the different EPDMs. For all EPDM compositions investigated, the network density increases linearly with the peroxide content up to at least 5 phr peroxide. These results are consistent with a simple additivity model with a constant entanglement density D_{EN} and a chemical cross-link density D_{CC} proportional to the peroxide content p. Both the entanglement and the chemical cross-link density further depend on the diene content d.

$$D_{tot}(d,p) = D_{EN}(d) + D_{CC}(d,p) \tag{3}$$

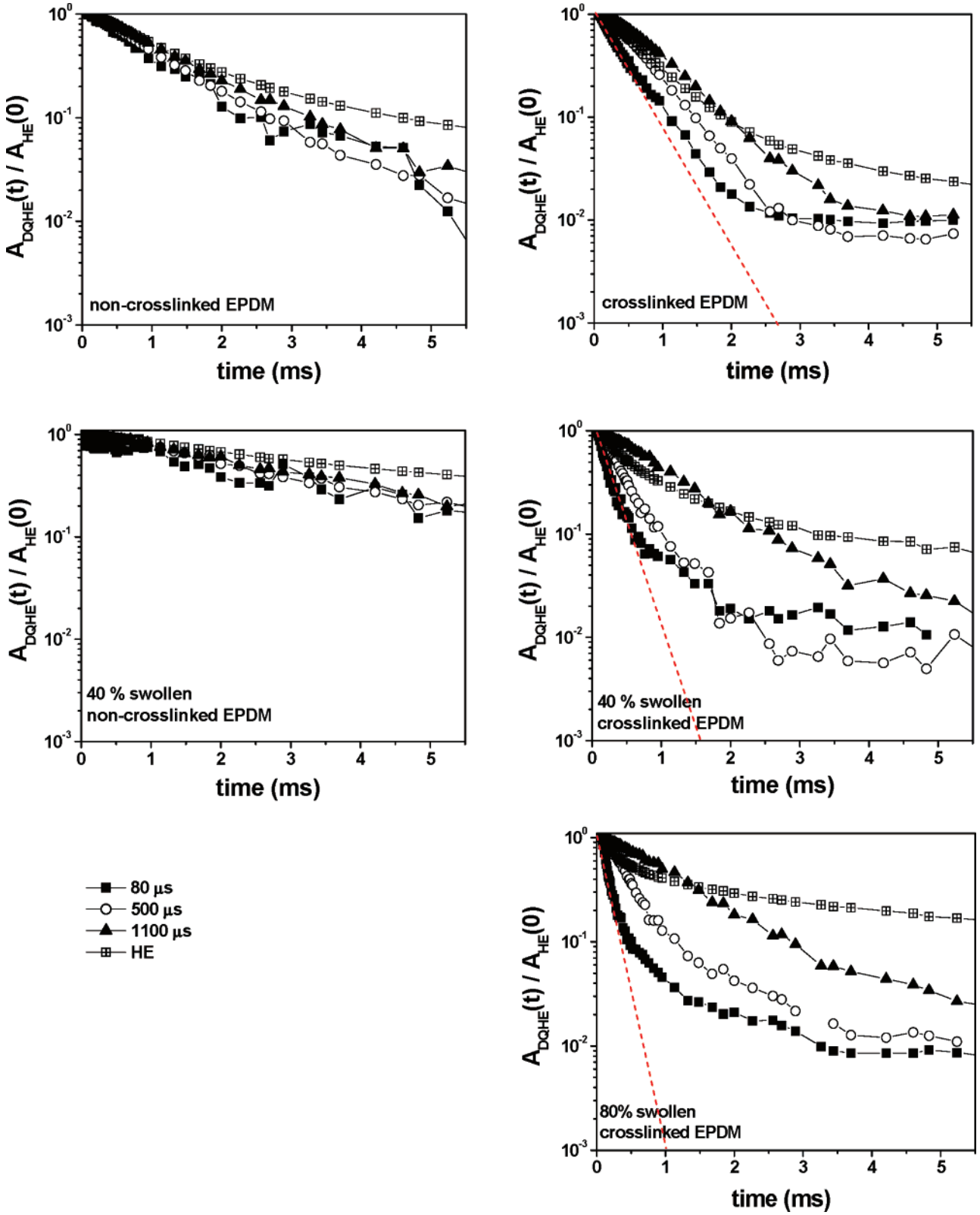

Figure 5. T_2 relaxation decays measured with Hahn-echo and DQ-filtered Hahn-echo pulse sequences for non-cross-linked EPDM with 9% ENB and 5 phr peroxide before and after cross-linking and swelling. The decay amplitude is normalized to its value at time zero. The slopes of the initial parts of the decays at short τ_{EX} are shown by the dotted lines.

Extrapolation of D_{tot} to zero peroxide yields the entanglement density D_{EN}, which is quite similar for the various EPDMs as expected. The entanglement densities are in the range 200−240 mmol/kg, which agree with previous NMR studies and are also consistent with the outcome of other studies based on rheology, neutron scattering, and mechanical properties.[30−32] Entanglements in EPDM contribute significantly to the total network density and consequently to the related macroscopic properties. The lowest value of D_{EN} is found for EPM without diene because this polymer has the most flexible chain due to the absence of the rigid diene monomer. The small differences in D_{EN} for the four EPDM grades with diene are caused by

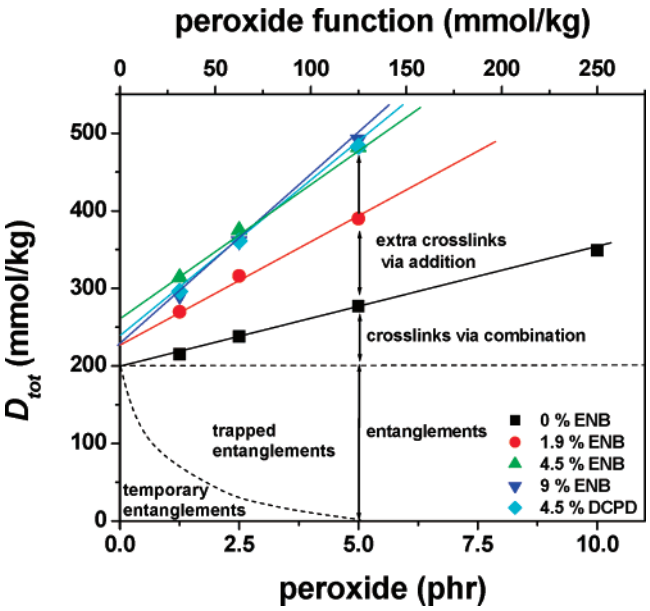

Figure 6. Total network cross-link density D_{tot} in peroxide-cured EPDM as a function of peroxide content. The contribution of different types of network junctions to the total cross-link density is described in the text.

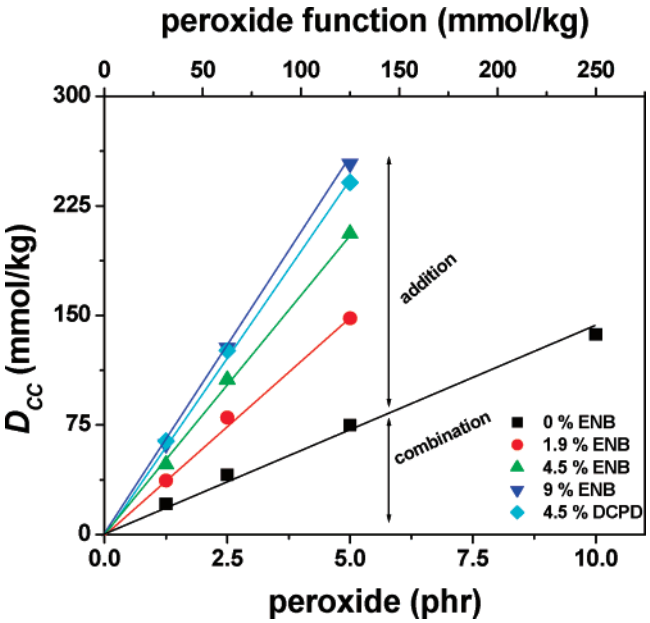

Figure 7. Density of chemical cross-links D_{CC} in peroxide-cured EPDM as a function of peroxide content.

differences in both diene and ethylene contents, resulting in subtle differences in the conformational states of the rubber chains.

3.3. Combination vs Addition. 3.3.1. ^{1}H NMR Transverse Relaxation. The difference between the total network density D_{tot} at any given peroxide content and the intercept, representing the entanglement density D_{EN} in Figure 6, represents the number of the chemical cross-links formed D_{CC} (Figure 7). According to the generally accepted reaction scheme as presented in Figure 2, two types of chemical cross-links are formed in the peroxide-cured EPDM, i.e., one type via combination of peroxide-induced EPDM macroradicals and the other one via addition of the macroradicals to the residual double bonds of the termonomer. Since EPM does not contain any unsaturation, peroxide cross-linking occurs only via the combination route. The enhanced chemical cross-link density determined for EPDM relative to

Table 2. Peroxide Efficiency and Diene Third Monomer Conversion and the Number of Addition Cycles for Cross-Linking of EP(D)M

peroxide content (phr)	diene type and content	peroxide efficiency (%)	diene conversion (%)	no. of addition cycles
1.25		38		
2.5	0% ENB	52		
5		53		
10		49		
1.25		99	9	1.9
2.5	1.9% ENB	127	29	1.2
5		113	47	1.5
1.25		157	8	0.9
2.5	4.5% ENB	173	19	0.8
5		165	36	0.8
1.25		198	6	0.6
2.5	9% ENB	207	12	0.6
5		203	24	0.6
1.25		181	11	0.7
2.5	4.5% DCPD	192	25	0.7
5		186	47	0.7

that for EPM (compare slopes in Figure 7) indicates that both types of cross-links are formed in EPDM. In principle, the two types of chemical cross-links are additive since all addition reactions generate new radicals, which eventually are all terminated via combination reactions. At low termonomer content, the density of cross-links via combination is probably independent of the termonomer content. Then, the chemical cross-link density $D_{CC}(d,p)$ in eq 3 can be linearly decomposed into a term resulting from combination $D_{CC,comb}(p)$, depending on the peroxide content p only, and an addition term $D_{CC,add}(d,p)$, which additionally depends on the termonomer content d, as:

$$D_{CC}(d,p) = D_{CC,comb}(p) + D_{CC,add}(d,p) \qquad (4)$$

Note that both terms are linearly dependent on the peroxide content. According to eq 4, the amount of cross-links formed via addition can be obtained by subtracting the density of chemical cross-links formed via combination for EPM from that of the total chemical cross-link density of EPDM cured with the same amount of peroxide. Figure 7 shows that increasing the ENB level results in increased contribution through addition type to the total cross-link density.

On comparison of the obtained chemical cross-link density with the initial peroxide content, the peroxide-cross-linking efficiency for EP(D)M can be calculated, which is defined as the number of cross-links formed per peroxide functionality (Table 2). All calculations are performed in millimoles per kilogram of the compound, with the peroxide being bifunctional and being used as a 40% masterbatch. The peroxide-cross-linking efficiencies are more or less constant for a given type of EP(D)M. For EPM it amounts to 50%, which is similar to values obtained via low molecular weight model experiments.[33] It indicates that only 50% of the original peroxide functions is effectively used for cross-linking; the other 50% of the peroxide functions reacts toward nonelastically active products. Although the presence of a diene termonomer is not a prerequisite for peroxide cross-linking, it does provide a significant increase of the peroxide cross-linking. Radicals formed via the addition reaction create new macroradicals that produce other cross-links without radical destruction, which yields an efficiency higher than 100%. Clearly, increasing the ENB content of EPDM results in increased peroxide-cross-linking efficiency, although at higher ENB contents the increase levels off.

From the slopes in Figure 7, it is concluded that 4.5% DCPD containing EPDM has similar reactivity as 9% ENB containing

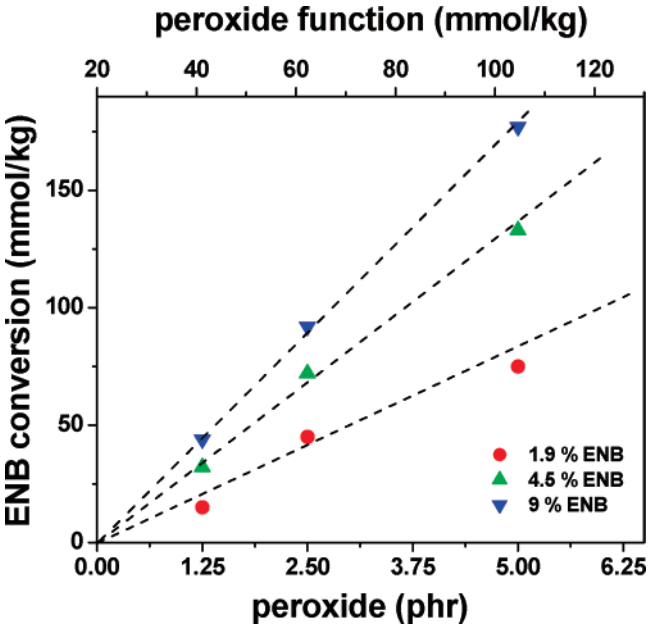

Figure 8. The conversion of ENB estimated from T_2 relaxation in peroxide-cured EPDM as a function of peroxide content calculated from NMR relaxometry.

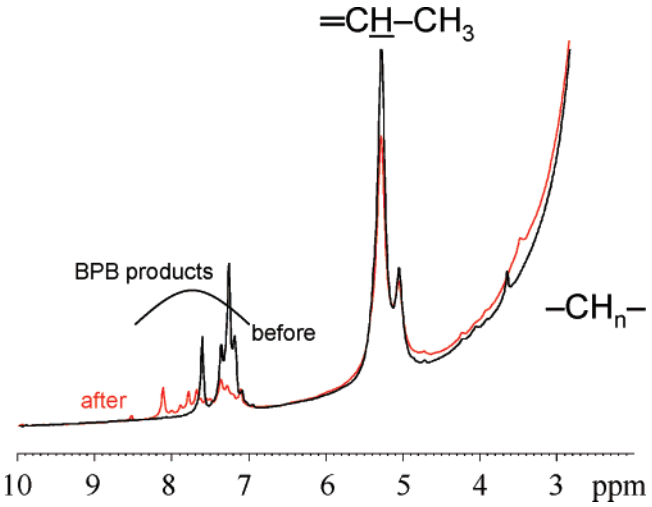

Figure 9. MAS ^{1}H NMR spectra of peroxide-cured EPDM (9% ENB and 5 phr peroxide) before and after cross-linking.

EPDM, which indicates that DCPD is almost twice as efficient in peroxide cross-linking than ENB. This is in fair agreement with previous studies.[34] The number of EPDM macroradicals which are actually formed can be calculated using the amount of peroxide functionality in millimoles per kilogram of EPDM and the peroxide-cross-linking efficiency of EPM. Combining this number with the number of cross-links formed via addition allows the calculation of the number of addition cycles per EPDM macroradical formed. The data given in Table 2 are rather low (<2), indicating that termination of the free-radical reaction sequence by combination is relatively fast compared to the cross-link formation. From the data shown in this table, the ratio of DCPD versus ENB conversion can be calculated. DCPD conversion is 1.3 times higher than that of ENB in similar recipes, which is in perfect agreement with the known ratio for cross-linking.[34]

3.3.2. Chemical Conversion of Diene Third Monomer. Comparison of the cross-link density via addition (Figure 8) with the initial termonomer content (Table 1) allows the calculation of the molar diene conversion (Table 2). Obviously,

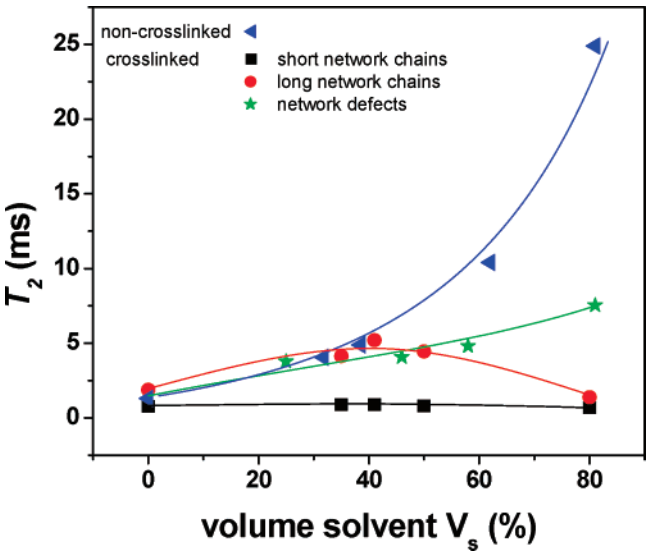

Figure 10. T_2 values characterizing the relaxation components of the T_2 decay vs the amount of solvent in swollen peroxide-cured EPDM (9% ENB and 5 phr peroxide). The components are tentatively assigned to short and long network chains and network defects as discussed in the text.

Table 3. Comparison of ENB Conversion upon Peroxide Cross-Linking of 9% ENB Containing EPDM Obtained from ^{1}H NMR T_2 Relaxometry, MAS ^{1}H NMR Spectroscopy, and FT-Raman Spectroscopy

peroxide content (phr)	^{1}H NMR relaxation (%)	^{1}H NMR spectroscopy (%)	Raman spectroscopy (%)
1.25	6	6	5
2.5	12	10	12
5	24	28	24

the higher the peroxide content the higher the diene conversion. For 1.9% ENB containing EPDM, the ENB conversion is far from complete (<50%), and at higher ENB content, the conversion is even lower (<40%). In other words, a major part of the diene is not used during peroxide cross-linking of EPDM. The residual diene content after peroxide cross-linking is of practical importance, since it increases the sensitivity to hot-air aging.

The MAS ^{1}H NMR spectra of the EPDM samples are dominated by the signals of aliphatic protons of the EPM backbone around 1 ppm (Figure 9). At large magnification of the spectra, the resonances of the vinyl protons of ENB as well as the aromatic protons of the peroxide are seen in the spectral range of 4−6 ppm and 7−9 ppm, respectively. Comparing the spectra of EPDM with 9% ENB before and after cross-linking suggests that the peroxide has been largely converted; the remaining aromatic signals are related to the aromatic ketone and alcohols, which are formed upon decomposition. The intensity of the unsaturated ENB resonances decreases as a result of the addition of the EPDM macroradicals to the unsaturation, which allows the determination of the ENB conversion. Figure 9 shows that for the EPDM sample with 9% ENB and 5 phr peroxide the ENB conversion estimated from the MAS ^{1}H NMR spectrum is approximately 30%. This value may be compared with the ENB conversion determined from the T_2 relaxation experiments, as discussed above. In addition, the diene conversion has also been determined via FT-Raman spectroscopy. The ENB conversion values, which are determined by these three methods for EPDM vulcanizates with the highest amount of ENB, are given in Table 3. The results of all the three methods are in good agreement. Thus, it can be concluded that the T_2

Table 4. Results of the DQ-Filtered HEPS Experiments for a Sample with the Highest Cross-Link Density(9% ENB Containing EPDM with 5 phr Peroxide)[a]

	volume of solvent		
excitation time	0%	40%	80%
τ_{short} (80 μs)	394 (4.1)	201 (10.2)	144 (22.3)
τ_{max} (500 μs)	683 (18.2)	382 (21.5)	431 (20.9)
τ_{long} (1100 μs)	954 (9.7)	1130 (9.3)	1259 (9.9)

[a] The mean decay time and the initial amplitude of the decay in the DQ-filtered experiment are normalized to their values measured by HEPS without the filter. T_2 is given in microseconds and the fraction in parentheses is in percentage.

relaxation method is a reliable tool for quantifying a series of network characteristics of the cross-linked rubber.

3.4. Enhanced Distinction between Network Chains and Defects in Swollen Cross-Linked EPDM. The largest distinction in the mobility of network chains and defects is observed for swollen samples. Swelling has two opposite effects on the chain mobility within the affine part of the rubber network. On one hand, it enhances the mobility by diminishing the density of temporary chain entanglements. On the other hand, it stretches the network chains and, in this way, increases the anisotropy of the network chain motions.[35] Under mild swelling conditions, the former occurs, but under extensive swelling conditions, the stretching prevails. Network defects, such as chain segments not connected to the network on both sides, do not take part in the stretching and become only more mobile upon swelling.

The contribution of the temporary chain entanglements to the total network density is usually evaluated by comparing the network density for samples in the swollen and in the solid (nonswollen) state.[13,36,37] T_2 was investigated as a function of the solvent content for the non-cross-linked and for the highly cross-linked EPDM (Figure 10). For the non-cross-linked EPDM, T_2 shows a monotonous increase in value versus the volume fraction of tetracholoroethane, reflecting the increasing mobility of the chains. The trend for the cross-linked EPDM is more complex. Analyzing the observed Hahn-echo decay in terms of the three components, it was found that the shortest T_2 component is hardly affected by swelling while the longest T_2 component shows a monotonous increase in value like the non-cross-linked EPDM. The intermediate T_2 component, associated with long network chains, initially increases up to a solvent content $V_s \approx 40$ vol %, where it reaches a maximum, and then decreases upon further increase of the amount of swelling solvent. The three trends are consistent with the expected motional anisotropy of the respective short network chains, network defects, and long network chains in a heterogeneously cross-linked network. Strongly cross-linked regions cannot swell, so the chain mobility does not change, whereas the network defects become increasingly mobile with increasing solvent content. The trend observed for the intermediate T_2 component, tentatively assigned to long network chains in less cross-linked regions, reflects the changing balance between the above mentioned disentangling versus stretching effects by swelling. At a volume fraction of the solvent of approximately 40%, the network density is mainly composed of chemical cross-links and trapped chain entanglements. The density of temporary entanglements in the cross-linked samples can be estimated by subtracting the network density in partially swollen samples from that of nonswollen vulcanizates. The main contributions to the total network density for the 9% ENB containing EPDM cross-linked with 5 phr peroxide are those of the chemical cross-links and the trapped chain entanglements. For low cross-link densities, the temporary chain entanglements provide the dominant contribution to the total network density. At the equilibrium swelling degree, the fraction ($\approx$7%) of the long T_2 relaxation component can be used as a measure of the fraction network defects.

To resolve the effect of swelling on the mobility of the short and long network chains as well as the network defects more clearly, DQ-filtered T_2 measurements have been performed on the swollen samples and the results have been compared with those on the nonswollen rubbers discussed above (Figure 5). Table 4 presents the effective relaxation times of the DQ-filtered T_2 decays measured at excitation times of 80, 500, and 1100 μs and solvent fractions of 0, 40, and 80 vol %. The shape of the DQ-filtered decays of the cross-linked EPDM depends largely on the excitation time and differs from that of the overall Hahn-echo decay (Figure 5). At long DQ-filter time, τ_{EX}, the Hahn-echo decay is slower and at a short filter time, the decay is faster than the nonfiltered overall decay (Figure 5 and Table 4). The slow component at long excitation time is observed to become even slower upon swelling, whereas the initial decay rates at short excitation time increase with increasing solvent amount. The latter is caused by an increase in the anisotropy of the chain motions as a result of chain stretching upon swelling, which is also reflected by an increase in the amplitude of the DQ signal. Swelling-induced changes in the decays are more pronounced for cross-linked EPDM compared to non-cross-linked EPDM. This suggests that the network structure of the cross-linked samples is far more heterogeneous than the entangled EPDM chains in the virgin rubber. Thus, the results

Table 5. Physical Properties of Peroxide-Cured EP(D)M

diene type and content (%)	peroxide content (phr)	torque (N m)	hardness (ShA)	elongation at break (%)	modulus 100% (MPa)	CS 23 °C (%)	CS 70 °C (%)	tensile strength (MPa)	tear strength (N)
	1.25	0.23	29		0.6	40	68		8.4
0 ENB	2.5	0.48	36	1050	0.7	24	42	3.0	10.3
	5	0.77	41	370	0.9	13	19	1.4	9.6
	10	0.95	45	250	1.0	6	10	1.4	9.6
	1.25	0.72	45	580	1.0	14	25	2.7	12.0
1.9 ENB	2.5	1.07	48	340	1.1	9	15	2.2	11.5
	5	1.48	52	167	1.3	5	7	1.9	10.1
	1.25	1.11	49	390	1.1	7	11	2.0	11.8
4.5 ENB	2.5	1.42	51	200	1.3	3	5	1.7	11.1
	5	1.92	56	120	1.6	2	3	1.7	10.2
	1.25	0.94	46	440	1.0	7	11	2.9	11.2
9 ENB	2.5	1.37	50	230	1.4	3	4	2.5	11.0
	5	2.02	57	90	1.8	1	2	1.6	9.3
	1.25	0.83	46	420	1.1	10	15	4.1	13.2
4.5 DCPD	2.5	1.28	50	210	1.3	5	7	2.4	11.4
	5	1.88	56	110	2.0	2	3	2.0	9.3

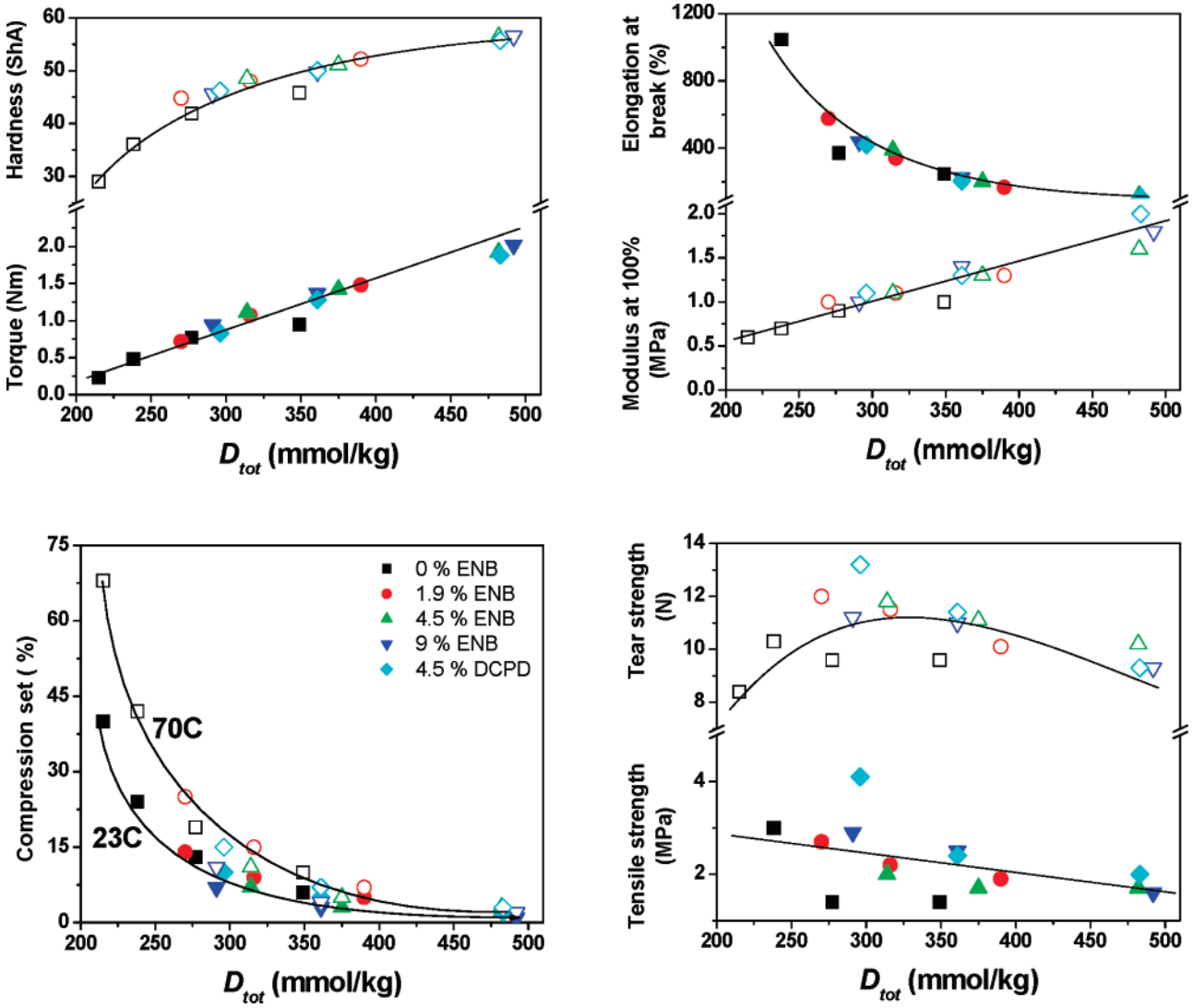

Figure 11. Correlation of rheometer torque, hardness, elongation at break, modulus at 100% elongation, compression sets at 23 and 70 °C, tensile strength, and tear strength with the total network cross-link density determined by the T_2 relaxation method.

of the DQ-filtered HEPS experiments support the assignment of the short and long T_2 relaxation components to the network chains and network defects, respectively, for swollen EPDM vulcanizates. DQ-filtered T_2 relaxometry is a powerful tool to resolve components with different mobilities in a heterogeneous rubber network. However, quantitative analysis of this experiment in relation to the network heterogeneity is hampered by a number of issues that have been recently discussed.[28]

3.5. Correlation of the Network Density with Mechanical Properties. In general, the physical properties of a cross-linked rubber depend not only on the cross-link density but also on the details of the curing. The factors contributing from the latter are the nature of the chemical bonds formed between the chains (for example sulfur bridges in sulfur vulcanisates vs C−C bonds in peroxide cures) and the functionality of the cross-links. Another factor is attributed to the differences in network heterogeneity, i.e., distribution of the cross-links and defects in the network.[38,39] The results of the present NMR study suggest significant network heterogeneity in peroxide-cured EPDMs. Therefore, the relationship between the average cross-link density, as determined by NMR, and the physical properties is not always straightforward. Nevertheless, some correlation can be established.

Common rubber properties, such as hardness, torque, elongation at break, modulus at 100%, and compression sets at 23 and 70 °C, have been measured for the complete set of peroxide-cured EPDM samples (Table 5). Even across the series with different diene and peroxide contents these mechanical properties correlate well with the total network density (Figure 11) in a way consistent with existing network models. Apparently, the network density calculated from T_2 relaxometry has a real physical meaning and is relevant for the macroscopic properties of the cross-linked EPDM rubbers. The rheometer torque correlates with the total network density in a linear fashion, which is in agreement with a previous real-time NMR study, and supports the use of rheometer torque in rubber technology.[40] The same holds for the modulus at 100%, which is consistent with the standard rubber elasticity theory. The elongation at break and the compression sets at 23 and 70 °C decrease upon increasing cross-link density although in a nonlinear fashion in agreement with general experience in rubber technology. The poor correlation between the tensile strength at break and the tear strength and the cross-link density is probably due to the defects or imperfections in the network in combination with the complex origin of the ultimate mechanical properties.

4. Conclusion

Applying T_2 relaxometry to a series of peroxide-cured EP(D)M samples with different diene and peroxide levels has allowed a quantitative determination of the total cross-link

density. The results presented in this work contribute to a better understanding of the elastomer materials. The respective contributions from temporary and trapped chain entanglements as well as two types of chemical cross-links originating from either combination of macroradicals or addition of macroradicals to the double bonds of the EPDM diene termonomers have been resolved. The peroxide-cross-linking efficiency is ≈50%. The conversion of the diene is determined by both peroxide and diene contents with a maximum of 47% for 1.9% ENB containing EPDM and 24% for 9% ENB containing EPDM. The latter was found to be consistent with the diene conversion estimated from MAS ^{1}H NMR spectroscopy and Raman spectroscopy. The total network density, as determined from T_2 relaxometry, correlates well with several common physical properties measured for the peroxide-cured EP(D)M. Combined with NMR spectroscopy or spectral-editing filters, NMR relaxometry can therefore yield reliable network density information for individual components in rubber blends or filled rubbers with domain sizes below the resolution limit of the macroscopic techniques.

Acknowledgment. This work is part of the research program of the Dutch Polymer Institute (Project No. 511). The authors would like to thank Brahim Mezari (TU/e) for his assistance with the MAS NMR spectra, Hans Kranenburg (TU/e) for performing the Raman measurements, and Roger Timmerman from DSM Elastomers BV (Geleen) for supplying the series of EPDM vulcanizates used in this study and for the mechanical testing.

References and Notes

(1) Orza, R. A.; Magusin, P. C. M. M.; Litvinov, V. M.; van Duin, M.; Michels, M. A. J. *Macromol. Symp.* **2005**, *230*, 144.
(2) Baldwin, F. P.; Borzel, P.; Cohen, C. A.; Makowski, H. S.; Castle van de, J. F. *Rubber Chem. Technol.* **1970**, *43* (3).
(3) Vallat, M. F.; Ruch, F.; David, M. O. *Eur. Polym. J.* **2004**, *40*, 1575.
(4) Assink, R. A.; Gillen, K. T.; Sanderson, B. *Polymer* **2002**, *43*, 1349.
(5) Gotlib, Yu. Ya.; Lifshits, V. A.; Shevelev, V. A.; Lishanskii, I. A.; Balanina, I. V. *Polym. Sci. U.S.S.R.* **1976**, *18*, 2630.
(6) Fry, C. G.; Lind, A. C. *Macromolecules* **1988**, *21*, 1292.
(7) Fulber, C.; Demco, D. E.; Weintraub, O.; Blumich, B. *Macromol. Chem. Phys.*, **1996**, *197*, 581.
(8) Brereton, M. G. *Macromolecules* **1990**, *23*, 1119.
(9) Brereton, M. G. *Macromolecules* **1993**, *26*, 1152.
(10) Menge, H.; Hotopf, S.; Heuert, U.; Schneider, H. *Polymer* **2000**, *41*, 3019.
(11) Litvinov, V. M. *Spectroscopy of Rubbers and Rubbery Materials*; RAPRA: Shawbury, U.K., 2002; p 353 and references therein.
(12) Litvinov, V. M.; Dias, A. A. *Macromolecules* **2001**, *34*, 4051.
(13) Richter, D.; Farago, B.; Butera, R.; Fetters, L. J.; Huang, J. S.; Ewen, B. *Macromolecules* **1993**, *26*, 795.
(14) Munowitz, M.; Pines, A. Principles and Applications of Multiple-Quantum NMR. In *Advances in Chemical Physics*; Prigogine, I., Rice, S. A., Eds.; Wiley-Interscience: New York, 1987; Vol. 66, p 1.
(15) Saalwächter, K.; Ziegler, P.; Spyckerelle, O.; Haidar, B.; Vidal, A.; Sommer, J.-U. *J. Chem. Phys.* **2003**, *119*, 3468.
(16) Ba, Y.; Ripmeester, J. A. *J. Chem. Phys.* **1998**,*108*, 8589.
(17) Buda, A.; Demco, D. E.; Bertmer, M.; Blümich, B.; Litvinov, V. M.; Penning, J. P. *J. Phys. Chem. B* **2003**, *107*, 5357.
(18) Buda, A.; Demco, D. E.; Bertmer, M.; Blümich, B.; Reining, B.; Keul, H.; Höcker, H. *Solid State Nucl. Magn. Reson.* **2003**, *24*, 39.
(19) Buda, A.; Demco, D. E.; Blümich, B.; Litvinov, V. M.; Penning, J. P. *ChemPhysChem* **2004**, *5*, 876.
(20) Cherry, B. R.; Fujimoto, C. H.; Cornelius, C. J.; Alam, T. M. *Macromolecules* **2005**, *38*, 1201.
(21) Hedesiu, C.; Demco, D. E.; Kleppinger, R.; Adams Buda, A.; Blümich, B.; Remerie, K.; Litvinov, V. M. *Polymer* **2007**, *48*, 763.
(22) Rubber (vulcanized or thermoplastic): determination of tensile stress-strain properties, ISO 37. Rubber (vulcanized or thermoplastic): determination of compression set at ambient, elevated, or low temperatures, ISO 815 type B. Guide to the use of curemeters, ISO 6502. Shore A and Shore D hardness testing of rubber, DIN 53505.
(23) Cohen-Addad, J. P. *Prog. Nucl. Magn. Reson. Spectrosc.* **1993**, *25*, 1.
(24) Cohen-Addad, J. P. *Spectroscopy of Rubbers and Rubbery Materials*; RAPRA: Shawbury, U.K., 2002; p 291.
(25) Brereton, M. G. *Macromolecules* **1991**, *24*, 2068.
(26) Cohen-Addad, J. P.; Girard, O. *Macromolecules* **1992**, *25*, 593.
(27) Kulagina, T. P.; Litvinov, V. M.; Summanen, K. T. *J. Polym. Sci., Part B: Polym. Phys.* **1993**, *31*, 241.
(28) Litvinov V. M. *Macromolecules* **2006**, *39*, 8727.
(29) Beck, K.; Voda, A.; Bescher, M.; Peterseim, V.; Viol, M. *7th Fall Rubber Colloquium* 2007.
(30) Richards, J. R.; Mancke, R. G.; Ferry, J. D. *J. Polym. Sci., Polym. Lett. Ed. 2*, **1964**, *197*.
(31) Richter, D.; Farago, B.; Butera, R.; Fetters, L. J.; Huang J. S.; Ewen, B.; *Macromolecules* **1993**, *26*, 795.
(32) Richter, D.; Ewen, B.; Fetters, L. J.; Huang, J. S.; Farago, B. *Prog. Colloid Polym. Sci.* **1993**, *99*, 130.
(33) AKZO Chemicals Division, Rubber Chemicals, Cross-linking peroxides.
(34) Duin van, M.; Dikland, H. G. *Rubber Chem. Technol.* **2003**, *76*, 132.
(35) Mark, J. E.; Erman, B. *Rubberlike Elasticity: A Molecular Primer*; Wiley: New York, 1988.
(36) Cohen-Addad, J. P.; Domard, M.; Lorentz, G.; Herz, J. *J. Phys. Les Ulis, Fr.* **1984**, *45*, 575.
(37) Schmidt, C.; Cohen-Addad, J. P. *Macromolecules* **1989**, *22*, 142.
(38) Mark H. F. *Rubber Chem. Technol.* **1988**, *61*, G73.
(39) Gehman S. D. *Rubber Chem. Technol.* **1969**, *42*, 659.
(40) Litvinov, V. M.; Duin van, M. *Kautsch. Gummi Kunstst.* **2002**, *55*, 460.

MA071015L